Quantum-Geometric Meissner Effect in Magnetized Color Superconductors

Noriyuki Sogabe (The University of Osaka)

Oct 27, NFQCD 2026, YITP

arXiv:2609.07835

Joint work with Kazuya Mameda (Tokyo University of Science)

Color superconductivity in magnetic fields

- Color-electromagnetic mixing in color superconductors:

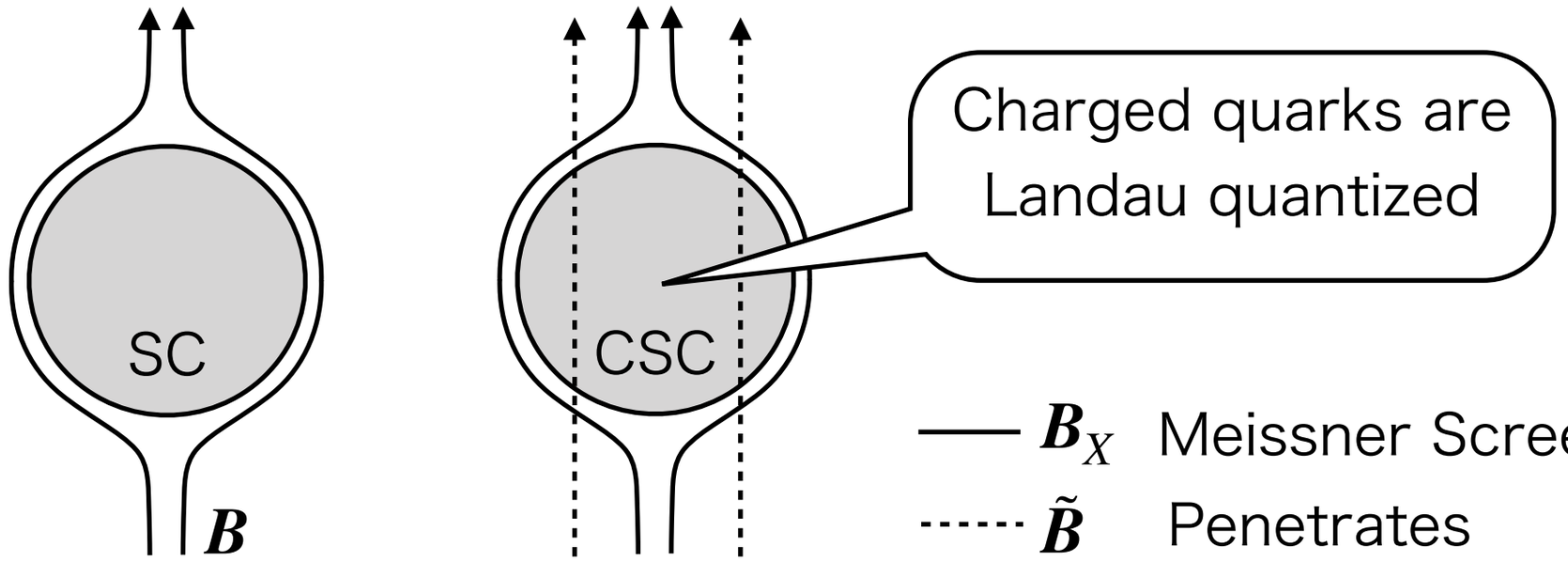

Alford, Berges, Rajagopal (2000)

- How does the Landau quantization (under $\tilde{\boldsymbol{B}}$) affect the Meissner response to $\boldsymbol{B}_X$?

Landau quantization of Weyl fermions

$$H = \boldsymbol{\sigma} \cdot (-\mathrm{i}\nabla - \tilde{q}\tilde{\boldsymbol{A}}), \quad H|u_{n,\lambda}\rangle = \varepsilon_{n,\lambda}|u_{n,\lambda}\rangle$$

$$(\tilde{\boldsymbol{B}} = \nabla \times \tilde{\boldsymbol{A}} = \tilde{B}\hat{\boldsymbol{z}})$$

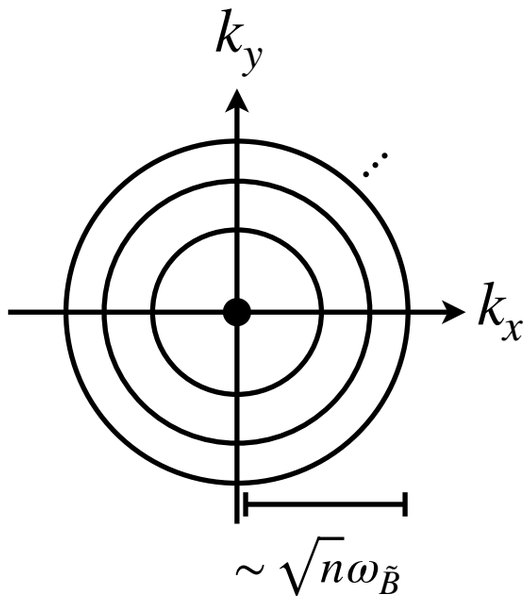

$$\omega_{\tilde{B}}^2 = 2|\tilde{q}\tilde{B}|$$

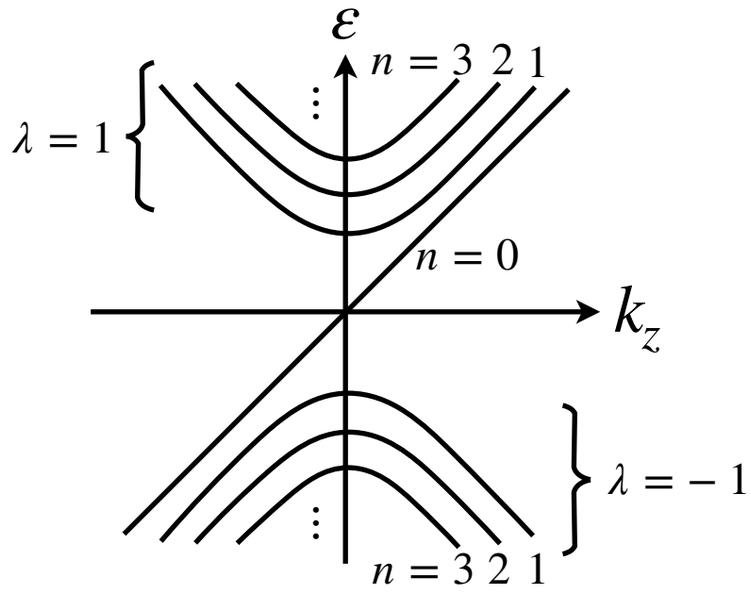

$$\varepsilon_{n,\lambda}(k_z) = \begin{cases} k_z, & n = 0, \\ \lambda\sqrt{k_z^2 + n\omega_{\tilde{B}}^2}, & n \geq 1. \end{cases}$$

Landau quantization quenches transverse dispersion

Transverse Meissner response under Landau quantization

- Polarization tensor Son and Stephanov (1999), Rischke (2003):

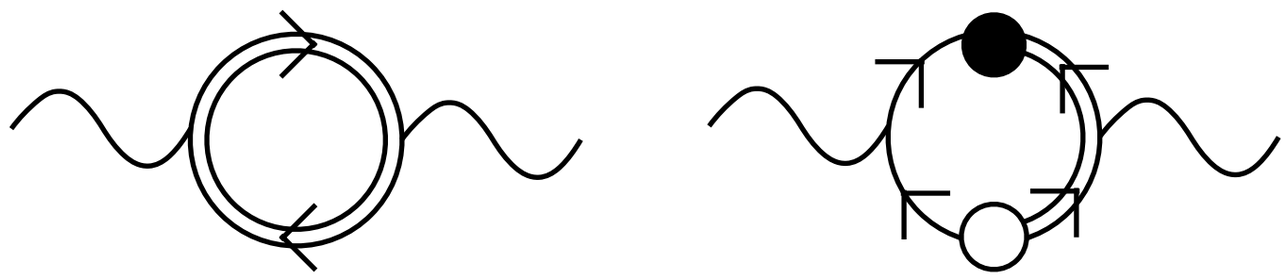

$$M^2 = \lim_{\boldsymbol{q}\to\boldsymbol{0}} \Pi^{\perp}(\omega = 0, \boldsymbol{q}) \qquad \Pi^{\perp} \equiv \frac{\Pi^{xx} + \Pi^{yy}}{2}$$

- Meissner response of magnetized CSC

  Conventional case: $M^2_{\mathrm{CFL}} \sim q_\Delta^2 N(0) \langle |\langle u_{\boldsymbol{k}}|\hat{\boldsymbol{v}}_\perp|u_{\boldsymbol{k}}\rangle|^2 \rangle_{\mathrm{FS}} \sim q_\Delta^2 \mu^2$ Sen (2015)

  (without Landau quantization)

  Landau quantization: intraband Fermi-velocity contribution vanishes

$$\langle u_{n,\lambda}|\boldsymbol{v}_\perp|u_{n,\lambda}\rangle = 0$$

  What sustains the transverse Meissner response?

Quantum geometry of wave functions

See the review by Gao, Nagaosa, Ni, Xu (2025)

- Quantum geometric tensor: characterizing the parameter dependence of wave functions, e.g., $\boldsymbol{k} \longmapsto |u_{\boldsymbol{k}}\rangle$:

$$Q_{ij}(\boldsymbol{k}) = \langle \partial_i u_{\boldsymbol{k}} | (1 - P_{\boldsymbol{k}}) | \partial_j u_{\boldsymbol{k}} \rangle = g_{ij}(\boldsymbol{k}) - \frac{\mathrm{i}}{2}\Omega_{ij}(\boldsymbol{k})$$

$$P_{\boldsymbol{k}} = |u_{\boldsymbol{k}}\rangle\langle u_{\boldsymbol{k}}| \qquad \partial_i \equiv \frac{\partial}{\partial k_i}$$

1) The quantum metric g_{ij} measures the distance between nearby states $|u_{\boldsymbol{k}}\rangle$ and $|u_{\boldsymbol{k}+\mathrm{d}\boldsymbol{k}}\rangle$
2) The Berry curvature Ω_{ij} describes the geometric phase

Quantum geometry of Landau-quantized Weyl fermions

- Quantum metric in the position-space formulation Bellissard, Elst, Schulz-Baldes (1994):

$$g_n^\lambda = a_{n,n+1}^{\lambda,+} + a_{n,n-1}^{\lambda,+} + a_{n,n+1}^{\lambda,-} + a_{n,n-1}^{\lambda,-}, \qquad a_{n,n'}^{\lambda\lambda'} \sim \frac{|\text{current matrix element}|^2}{(\text{energy difference})^2}$$

Transverse-current selection rule: $\Delta n = \pm 1$

- Topological bound:

$$g_n^\lambda \geq \frac{|\Omega_n^\lambda|}{2} = \frac{|C|}{\omega_{\tilde{B}}^2}$$

C : Chern number associated with the transverse Landau-level geometry

Lowest Landau level (LLL): $g_0^+ = \dfrac{|C|}{\omega_{\tilde{B}}^2}$ (saturation)

Meissner response in magnetized 2SC

Mameda and NS (2026)

- Nambu–Gor'kov mean-field action for $u_{\rm r}$-$d_{\rm g}$ pairing in 2SC
- Transverse Meissner response in the Landau-level basis

$$M^2(\tilde{B}) = \frac{q_\Delta^2 \omega_{\tilde{B}}^2}{4\pi} \sum_{n,n'} \sum_{\lambda,\lambda'} \int \frac{\mathrm{d}k_z}{2\pi} T_{nn'}^{\lambda\lambda'}(k_z) S_{nn'}^{\lambda\lambda'}(k_z)$$

Current matrix element:

$$T_{nn'}^{\lambda\lambda'}(k_z) = \frac{1}{2} \left| \langle u_n^\lambda(k_z) \,|\, \boldsymbol{\sigma}^\perp \,|\, u_{n'}^{\lambda'}(k_z) \rangle \right|^2$$

Quasiparticle distribution factor

$$S_{nn'}^{\lambda\lambda'}(k_z) \qquad (T = 0)$$

Quantum geometry and Meissner response

Mameda and NS (2026)

- Isolated Landau-Level limit $|\varepsilon_{n'}^{\lambda'} - \varepsilon_{n}^{\lambda}| \gg |\Delta|$
- Quantum-geometric Meissner response

$$M_{\mathrm{ILL}}^2(\tilde{B}) = \frac{q_\Delta^2 |\Delta|^2 \omega_{\tilde{B}}^2}{2\pi} \sum_{n=0}^{n_{\mathrm{F}}} \int \frac{\mathrm{d}k_z}{2\pi} \frac{\mathscr{G}_n^+}{E_n^+}$$

n_{F}: highest Landau level at the Fermi energy

E_n^+ : quasi-particle energy

$\mathscr{G}_n^+$: geometric factor related to the quantum metric

Saturation of the topological bound

Mameda and NS (2026)

- Strong-field (LLL-dominated) regime $\omega_{\tilde{B}} \gg \mu \Longrightarrow n_F = 0$

$$\mathscr{G}_0^+ \longrightarrow \frac{3}{2} g_0^+, \qquad \underbrace{g_0^+ = \frac{|C|}{\omega_{\tilde{B}}^2}}_{\text{saturation}}$$

- The transverse Meissner response is dominated by the LLL quantum metric, which saturates the Chern-number bound

$$M_{\mathrm{ILL}}^2 \longrightarrow \frac{3|C| q_\Delta^2 |\Delta|^2}{4\pi^2} \log \frac{2\omega_{\tilde{B}}}{|\Delta|}$$

$M_{2\mathrm{SC}} \sim |\Delta|$ rather than μ

- In lattice systems, the continuum Landau-level approximation breaks down at strong flux per unit cell Peotta and Torma (2015)

Crossover from conventional to quantum-geometric scaling

Mameda and NS (2026)

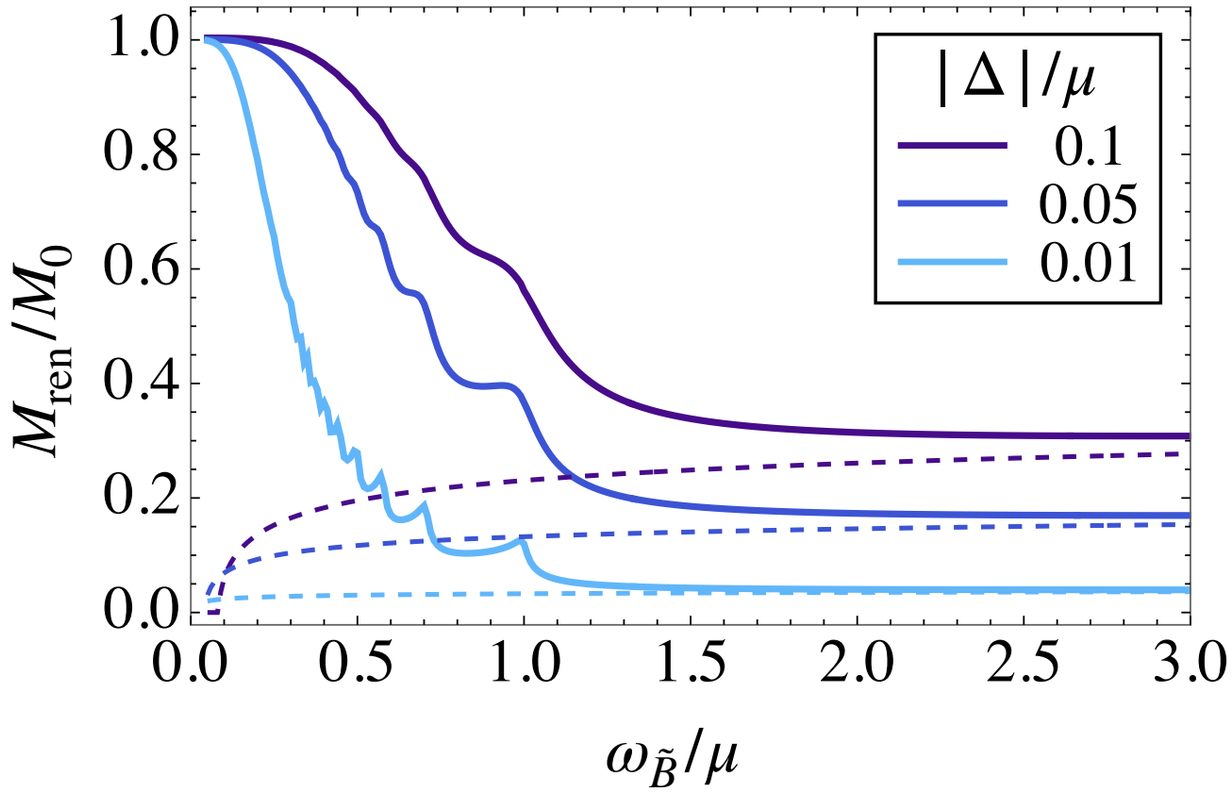

$$M_0 \equiv \lim_{\tilde{B}\to 0} M_{\rm ren}(\tilde{B}) \propto q_\Delta \mu$$

Solid: Full numerical results (renormalized)

Dashed: LLL contribution

conventional $M \propto \mu$ ⟷ quantum geometric $M \propto |\Delta|$

Implications for magnetars

Mameda and NS (2026)

- Magnetar quasi-periodic oscillations (QPOs): Observed in X-rays following giant flares.
- High-frequency QPOs (~kHz): Conventional scenarios require higher overtones, which may suffer from strong damping.
- Transverse perturbations along field lines:

$$w\,\partial_t^2\xi = T^{\parallel}\,\partial_z^2\xi, \qquad T^{\parallel} \propto B_{\rm core}M^2\,.$$

⟶ Propagation velocity $v^2 = \dfrac{T^{\parallel}}{w}$

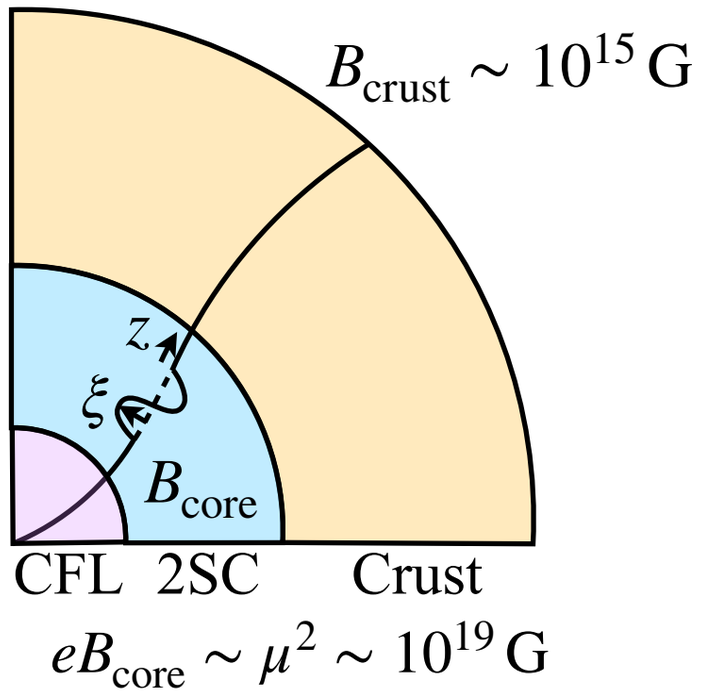

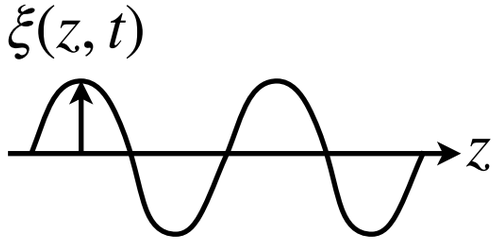

Quantum-geometric propagation scale

Mameda and NS (2026)

- Quantum-geometric propagation scale:

$$M_{\rm 2SC} \sim |\Delta| \ll M_{\rm CFL} \sim \mu \qquad\qquad v_{\rm Alfven} \ll v_{\rm 2SC} \ll v_{\rm CFL}$$

- Characteristic frequency of the 2SC layer

$$f_{\rm 2SC} \sim \frac{|\Delta|}{\mu}\frac{c}{L_{\rm 2SC}} \sim {\rm kHz} \qquad |\Delta|/\mu \sim 10^{-2}\text{-}10^{-1}, \qquad L_{\rm 2SC} \sim 1\text{-a few km}$$

Quantum-geometric scenario: A fundamental mode in the ~ 1 kHz range

Summary

Mameda and NS (2026)

arXiv:2609.07835

- **Quantum-geometric Meissner effect**: Landau quantization suppresses the conventional Fermi-velocity contribution $(M \sim \mu)$ to the transverse Meissner response, allowing the quantum-geometric contribution $(M \sim |\Delta|)$ to dominate.
- **Dominance of LLL quantum geometry**: In the strong-field regime, the Meissner response is dominated by the LLL quantum metric that saturates the Chern-number bound.
- **Implications for magnetar QPOs**: The suppressed transverse Meissner mass in 2SC creates an intermediate propagation scale that may support fundamental modes in the kHz range.